JOURNAL OF NEUROPHYSIOLOGY
Vol. 45, No. 3, March 1981. *Printed in U.S.A.*

Visual Response Properties of Neurons in Four Extrastriate Visual Areas of the Owl Monkey (*Aotus trivirgatus*): a Quantitative Comparison of Medial, Dorsomedial, Dorsolateral, and Middle Temporal Areas

JAMES F. BAKER, STEVEN E. PETERSEN, WILLIAM T. NEWSOME, AND JOHN M. ALLMAN

Divison of Biology 216-76, California Institute of Technology, Pasadena, California 91125

SUMMARY AND CONCLUSIONS

1. The response properties of 354 single neurons in the medial (M), dorsomedial (DM), dorsolateral (DL), and middle temporal (MT) visual areas were studied quantitatively with bar, spot, and random-dot stimuli in chronically implanted owl monkeys with fixed gaze.

2. A directionality index was computed to compare the responses to stimuli in the optimal direction with the responses to the opposing direction of movement. The greater the difference between opposing directions, the higher the index. MT cells had much higher direction indices to moving bars than cells in DL, DM, and M.

3. A tuning index was computed for each cell to compare the responses to bars moving in the optimal direction, or flashed in the optimal orientation, with the responses in other directions or orientations within ± 90°. Cells in all four areas were more sharply tuned to the orientation of stationary flashed bars than to moving bars, although a few cells (9/92) were unresponsive in the absence of movement. DM cells tended to be more sharply tuned to moving bars than cells in the other areas.

4. Directionality in DM, DL, and MT was relatively unaffected by the use of single-spot stimuli instead of bars; tuning in all four areas was broader to spots than bars.

5. Moving arrays of randomly spaced spots were more strongly excitatory than bar stimuli for many neurons in MT (16/31 cells). These random-dot stimuli were also effective in M, but evoked no response or weak responses from most cells in DM and DL.

6. The best velocities of movement were usually in the range of 10–100°/s, although a few cells (22/227), primarily in MT (14/69 cells), preferred higher velocities.

7. Receptive fields of neurons in all four areas were much larger than striate receptive fields. Eccentricity was positively correlated with receptive-field size ($r = 0.62$), but was not correlated with directionality index, tuning index, or best velocity.

8. The results support the hypothesis that there are specializations of function among the cortical visual areas.

INTRODUCTION

The discovery of a large number of extrastriate cortical visual areas has led to the hypothesis that each area performs its own set of functions in visual perception or visuomotor coordination (1–9, 35, 54, 58, 73, 75, 78, 91). The representations are most numerous and the amount of cortex devoted to these representations most extensive in animals apparently specialized for complex

uses of visual information, such as the cat (58, 75, 76) and various primates (1–9, 54, 78). Owl monkey visual cortex contains at least nine topographic representations of the visual field (3–8, 54) (see Fig. 1). We have studied functional localization in four extrastriate areas by making quantitative comparisons of the visual response properties of single neurons in the middle temporal (MT), dorsolateral (DL), dorsomedial (DM), and medial (M) areas. In this paper we report the response properties of neurons in these areas to direction of movement, bar orientation, single-spot, and random-dot stimuli. Rather than attempt to classify neurons into categories, we have developed a series of indices computed for each cell for directionality, tuning, and other parameters through which we have assessed the similarities and differences among the populations of cells recorded from MT, DL, DM, and M. Abstracts of this work have been published previously (11, 55, 59).

METHODS

Seven owl monkeys were surgically prepared and used in weekly recording sessions. The preparatory surgery was performed under aseptic conditions and general anesthesia (ketamine HCl, 25 mg/kg im, supplemented as needed). A stainless steel cylindrical chamber, 15 mm in diameter, with a threaded cap was positioned over an opening in the skull exposing extrastriate cortex and was cemented in place with Grip dental cement (L. D. Caulk Co., Milford, DE). Thorough removal of the periosteum and application of primer and cement over a large portion of the skull insured a strong bond. The chamber could be positioned for microelectrode penetrations nearly perpendicular to the cortical surface or for obliquely angled penetrations. After the chamber was in place, the exposed brain visible through the unopened dura mater was photographed for later reference. Within a few weeks a tissue growth covered the dura and obscured the cortex, and in some animals after several experiments it was necessary to remove this growth surgically so that microelectrodes could penetrate to the cortex without being damaged.

At the outset of each experimental session a monkey was tranquilized with Vetame (triflupromazine HCl, 5 mg/kg im initial session, tapered to 2 mg/kg in later sessions). Very small doses of Ketalar (ketamine HCl, 3-10 $mg \cdot kg^{-1} \cdot h^{-1}$ im) were used to maintain sedation throughout the 12- to 14-h session. The monkey's head was fixed in place with a circular clamp tightened around the recording chamber. This clamp was attached to a specially designed monkey chair in which the animal was restrained in the normal owl monkey posture. Owl monkeys, like other New World monkeys, squat rather than sit as do Old World monkeys, which possess ischial callosities; thus most commercially manufactured primate chairs are inappropriate for New World monkeys since they force the animal into an unnatural posture. The monkey was wrapped in a towel for warmth. The corneas, scleras, and eyelids were then topically anesthetized with a buffered solution of 0.5% dibucaine HCl, and the pupils were dilated with Cyclogyl (cyclopentolate 1%). After allowing the local anesthetic to take effect, the eyelids were retracted and held open with tape. Eye rings machined to fit the contour of the eye were cemented around the margins of the corneas with Histoacryl tissue adhesive (*n*-butyl cyanoacrylate, B. Braun, Melsungen, West Germany), thus fixing the animal's gaze.

Contact lenses of +4 diopters power were used to protect the corneas from drying and bring the eyes into focus on a tangent screen 28.5 cm away. Images of the optic disks were projected onto the tangent screen with an ophthalmoscope (22), allowing the experimenters to check the focus and to bring the eyes into binocular alignment. Correct binocular alignment was achieved by adjusting ball joints to which the eye ring stems were attached until the optic disks were projected at the same height on the screen and 40° apart. Superimposition of monocular receptive fields confirmed that 40° separation was the normal physiological position in all but one animal, for which 36–37° separation superimposed monocular fields. Care was taken not to torque the eyes or put pressure on the globe when positioning the eyes. Optic disk alignment was checked periodically during the session and at the end of the session before the eye rings were gently removed. The corneas remained in good condition throughout the course of these experiments. The owl monkey, like the owl, tends to move its eyes very little; the attachments of the extraocular muscles are placed far back on the globe relative to other monkeys and have a poor mechanical advantage. Thus this system provided good ocular stability.

The recording chamber was opened and cleaned with a mild solution of hydrogen peroxide (0.1%), then filled with warm mineral oil and sealed by the attachment of the microelectrode positioning device. This device could be rotated on the chamber and the microelectrode advance mechanism was mounted on a calibrated slide, thus establishing a polar coordinate system. Glass-insulated platinum-iridium microelectrodes were used to penetrate the dura and record the activity of single

neurons (85). All materials coming into contact with the interior of the recording chamber were sterile.

Initial microelectrode placements in an experimental animal were guided by the need to construct a map of the exposed extrastriate cortex based on the visual-field positions of single-unit and background responses. Progressions of receptive fields from the upper visual quadrant to the lower quadrant and reversals of progressions at the vertical and horizontal meridians were used to locate the extrastriate areas and their boundaries by comparison with the known organization of owl monkey visual cortex shown in Fig. 1. Usually, two or three extrastriate areas were studied in an animal. Most units could be unambiguously assigned to a particular area. However, some units (126/480) were recorded at area boundaries or near uncertain area boundaries, and these were excluded from the data analyses reported here. Assignment of units to extrastriate areas was based solely on receptive-field progressions and/or histological reconstructions, and all units that could be classified were included in the data analyses.

The visual responses of extrastriate units were studied both qualitatively and quantitatively. A unit was considered to be isolated well enough for study when its impulse could be made to trigger an oscilloscope sweep reliably, as determined by stored wave form superimposition. When a unit was isolated, a suitable stimulus was found and the receptive field was plotted with hand-controlled stimuli while listening to the unit's activity over an audio monitor. An estimate was made of the unit's preferred stimulus parameter values, then quantitative study was begun using computer-controlled stimuli. After quantitative study, a final qualitative assessment was made to reconfirm the unit's characteristics.

Quantitative evaluation of unit properties was done by computer routines developed for a Data General Nova 2 computer (primarily by Francis Miezin). These programs controlled a rear-projection optic stimulator equipped with galvanometer mirrors, stepping motors, and an electric shutter. The computer operated these peripheral devices to control stimulus orientation, direction of movement, velocity, shape, and size. Normally, one of these parameters was varied in a pseudorandom sequence of 8–12 values, and the sequence was presented 5 times. Repeated pseudorandomized presentations were necessary to avoid possible habituation effects (35) and to minimize the effects of trial-to-trial variability in extrastriate unit responses. The interstimulus interval was 6 s, with the 3 s immediately preceding the stimulus presentation used for estimating spontaneous activity. Parameters not being studied were held at their estimated best value. When a unit responded well to a light- or dark-bar stimulus, the effect of varying the orientation and direction of a moving bar was studied first. The responses were displayed as they occurred on an oscilloscope as peristimulus time histograms. As soon as the five runs of the stimulus sequence were completed, the orientation tuning of the unit was displayed on a polar plot. The optimal orientation was then used when studying other parameters with elongated stimuli. Responses were studied to different velocities, directions of spot movement, bar lengths, widths, spot sizes, and random-dot stimuli. The random-dot stimuli consisted of a fixed 40° area centered on the receptive field and in which randomly spaced small spots (density, 10%; 0.5- or 1.3°-diameter spots) moved in the same direction at a uniform velocity. In addition to the immediate display of results, the time of occurrence of each impulse and the stimulus parameter values were stored on magnetic disks for later analysis.

A second set of programs was used for off-line data analysis. A neuron's spontaneous firing rate (spikes per second) in the 3-s interval before stimulus presentation was subtracted from its firing rate during stimulus presentation to yield the net response rate for a single sweep. The stimulus sweep was adjusted to extend slightly beyond a unit's receptive-field boundaries. The average net response rate over the five identical sweeps in the repeated pseudorandom sequence was used in subsequent calculations to compare responses at different parameter values and, after normalizing the data, to compute various indices of stimulus selectivity.

The programs then classified these indices and other unit data into groups by extrastriate areas, and statistical tests (F tests, t tests, linear regression, correlations) were performed on the grouped data to determine whether data were signficantly different across areas and which indices were correlated within an area or across all areas.

The physiologically derived maps of extrastriate cortex were confirmed by histology done on three animals. Small electrolytic lesions (10 μA for 10 s) were placed at one to three locations along selected penetrations. At the termination of the final unit-recording session the monkey was deeply anesthetized with a lethal dose of sodium pentobarbital and then perfused with 0.9% saline followed by 3.7% formaldehyde in 0.9% saline. The head was mounted in the experimental position, and marking pins were placed at designated coordinates to aid electrode track reconstruction. The brain was removed from the skull, photographed, and placed in 30% sucrose in Formol-saline. Alternate 40-μm frozen sections were stained with cresyl violet for cell bodies and hematoxylin for myelin. The heavy myelination of

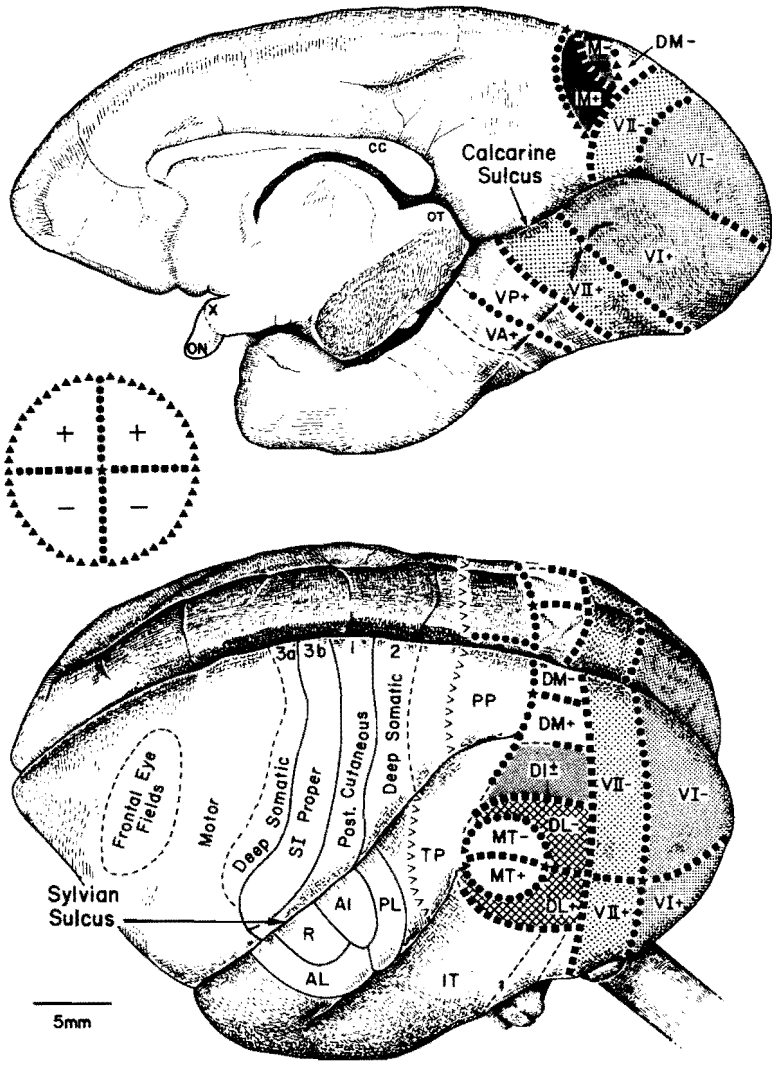

FIG. 1. Representations of the sensory domains in the cerebral cortex of the owl monkey. Above is a ventromedial view; below is a dorsolateral view. On the left is a perimeter chart of the visual field. Symbols in this chart are superimposed on the surface of the visual cortex. Pluses indicate upper-quadrant representations; minuses, lower quadrants; dashed lines, borders of areas that correspond to the representations of the relatively peripheral parts of the visual field, but not the extreme periphery. The row of Vs indicates the approximate border of visually responsive cortex. The dashed line broken by a question mark indicates an uncertain border. AI, first auditory area; AL, anterolateral auditory area; CC, corpus callosum; DI, dorsointermediate visual area; DL, dorsolateral crescent visual area; DM, dorsomedial visual area; IT, inferotemporal cortex; M, medial visual area; MT, middle temporal visual area; ON, optic nerve; OT, optic tectum; PL, posterolateral auditory area; PP, posterior parietal cortex; R, rostral auditory area; VA, ventral anterior visual area; VP, ventral posterior visual area; X, optic chiasm. The cortical visual areas were mapped by Allman and Kaas (3–8) and Newsome and Allman (54). The somatosensory areas were mapped by Merzenich et al. (51). The auditory areas were mapped by Imig et al. (38).

MT, visible even in unstained sections, was the most readily identified myeloarchitectonic feature (3). Histological reconstruction confirmed the area designations determined by receptive-field progressions.

RESULTS

Neurons in all four areas shared certain response properties. An appropriately sized bar of a particular orientation, direction, and

velocity of movement through a neuron's receptive field was nearly always an effective stimulus, although a few exceptions will be noted below. Hand-mapped receptive fields were homogeneously excitatory. Computer-controlled raster maps of 21 cells confirmed the homogeneity of the receptive fields, showing no strong inhibitory regions. In DM, M, and MT, responses for most cells summated for stimuli up to the length of the receptive field and were unaffected by further increases in length (60). In DL, the preferred stimulus length for 70% of the cells was much less than the length of the receptive field (60). The results are presented below as distributions of response properties rather than as arbitrary classes of cells. Most distributions were unimodal and thus did not provide the natural bases for class divisions. Exceptions included the flashed bar and random-dot response distributions; some cells in certain areas were unresponsive to these types of stimuli.

Responses to moving bars

The most important factors affecting the responses of the majority of extrastriate neurons studied were the direction and orientation of a moving stimulus. These were first assessed for each neuron with a bar stimulus oriented perpendicular to its direction of movement, which was swept through the receptive field in a pseudorandomly ordered sequence of 12 directions separated by 30° intervals that was repeated 5 times. This bar direction/orientation series was run on a total of 480 cells, 56 in M, 89 in DM, 80 in DL, 129 in MT, and 126 that could not be assigned to a particular area.

A neuron's spontaneous firing rate was subtracted from the mean firing rate during the stimulus presentation to obtain response rates, which were averaged for the five sweeps in a particular direction. Responses were normalized to a percentage of the maximum response and displayed as in Fig. 2, which shows responses as a function of bar stimulus direction for a cell in MT (top) and a cell in DM (bottom). Two response measures were calculated from these data: a direction index, which compared the response in the best direction of movement with the response in the direction 180° opposite, and a tuning index, which compared the response in the best direction with those to directions within ±90°. The formula used for calculating the direction index was 1 minus the

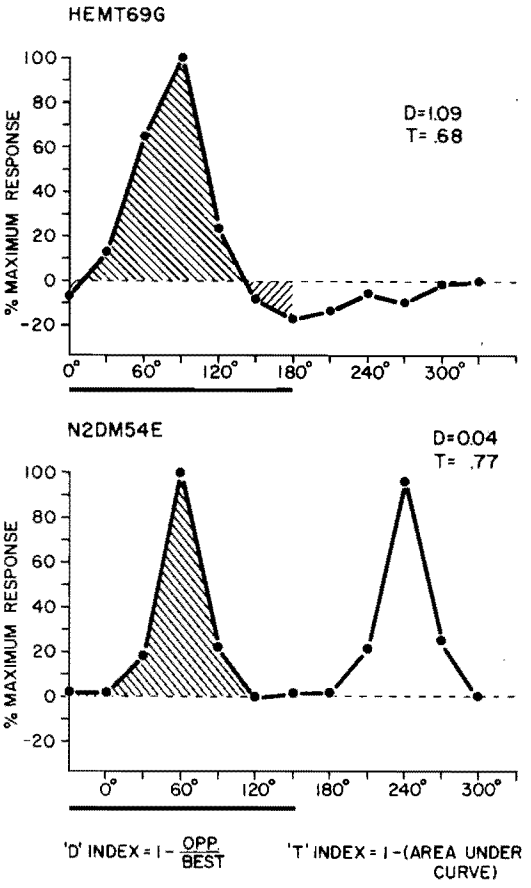

FIG. 2. Calculation of the direction and tuning indices for representative neurons from MT (top) and a neuron from DM (bottom). Directions of motion at which stimuli were presented are plotted horizontally. The neuronal response for stimuli moving in each direction as a percentage of the optimal response is plotted vertically. The illustrated response in each direction is the arithmetic mean of the individual responses to the five stimulus presentations. Formulas for computation of direction and tuning indices are given at the bottom. The shaded area for each response curve is the area under the curve computed for calculation of the tuning index. The direction index may be greater than 1 if spontaneous firing is inhibited by stimuli directed opposite to the optimum direction, as is the case for the upper neuron. In the calculation of the tuning index, if the spontaneous firing rate is inhibited in some of the directions within ±90° of the optimum, the area under the curve is the algebraic sum of the areas above and below the zero response level (areas of inhibition being negative). This situation obtains for the upper neuron.

ratio of the response in the 180° opposite direction to the response in the best direction. Thus for the cell illustrated at the bottom of Fig. 2, the ratio of opposite response to best response was almost 1 and the direction index almost zero. For the cell illustrated at the top of Fig. 2, the direction index was approximately 1, exceeding this value because spontaneous firing was inhibited in the opposite direction. Previously described direction-selective cells (12) would have high direction indices.

The distributions of direction indices for cells in the four extrastriate areas studied are shown in Fig. 3. Cells in M and DM had consistently low direction indices, while MT cells usually had high direction indices. The direction indices of DL cells varied widely.

The statistical test used was a one-way analysis of variance with comparisons being made between areas using Sheffe's multiple comparisons (62; see Fig. 3 for S values). We assumed that recordings made in the same area of different animals were from the same population.

The tuning index measured a cell's selectivity for the best direction of movement as compared with other directions within 90°. The normalized area under the tuning curve out to 90° on either side of the best direction (the shaded area in Fig. 2) was subtracted from 1 to yield the tuning index. The area measured was restricted to $\pm 90°$ so that the tuning for bidirectional and directionally selective cells could be measured on the same scale. The tuning index is close to 1 for sharply tuned cells and close to 0 for very broadly tuned cells. When spontaneous firing was inhibited in some of the relevant directions, the area under the curve was taken as the difference between the areas above and below the spontaneous level. This inhibition was uncommon and, when present, was usually weak. The distributions of tuning indices for M, DM, DL, and MT are illustrated in the histograms of Fig. 4. Although the differences are not as striking as for the direction index, an analysis of variance showed that DM cells were significantly more sharply tuned than M ($P < 0.02$), DL ($P < 0.01$), and MT ($P < 0.02$) cells. The average response magnitude and signal-to-noise ratios are shown in Table 1.

Two-dimensional plots of the cells' tuning

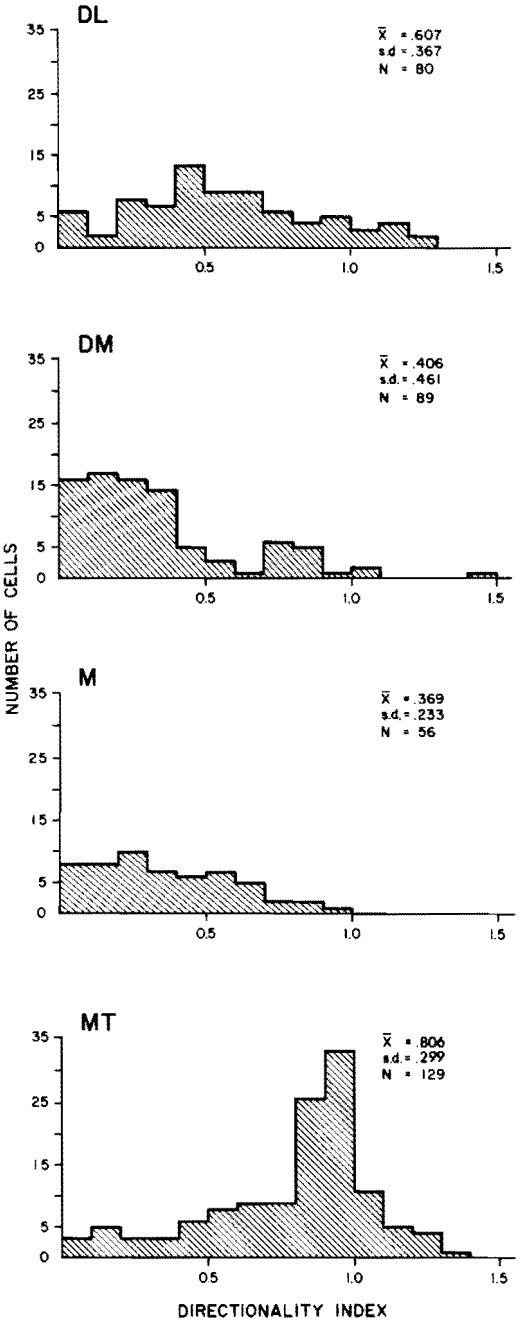

FIG. 3. Distribution of direction indices for DM, DL, MT, and M. MT neurons are strongly grouped near a direction index of 1.0, which differs markedly from the distributions present in DM, DL, and M. An analysis of variance was performed on these data (62). The value of S (Scheffe's multiple comparisons) for MT versus DM was 10.89; MT versus M was 9.37; MT versus DL was 3.5; P is very much smaller than 0.01 for the MT − DM and MT − M differences and less than 0.02 for the MT − DL differences (df = 3,351).

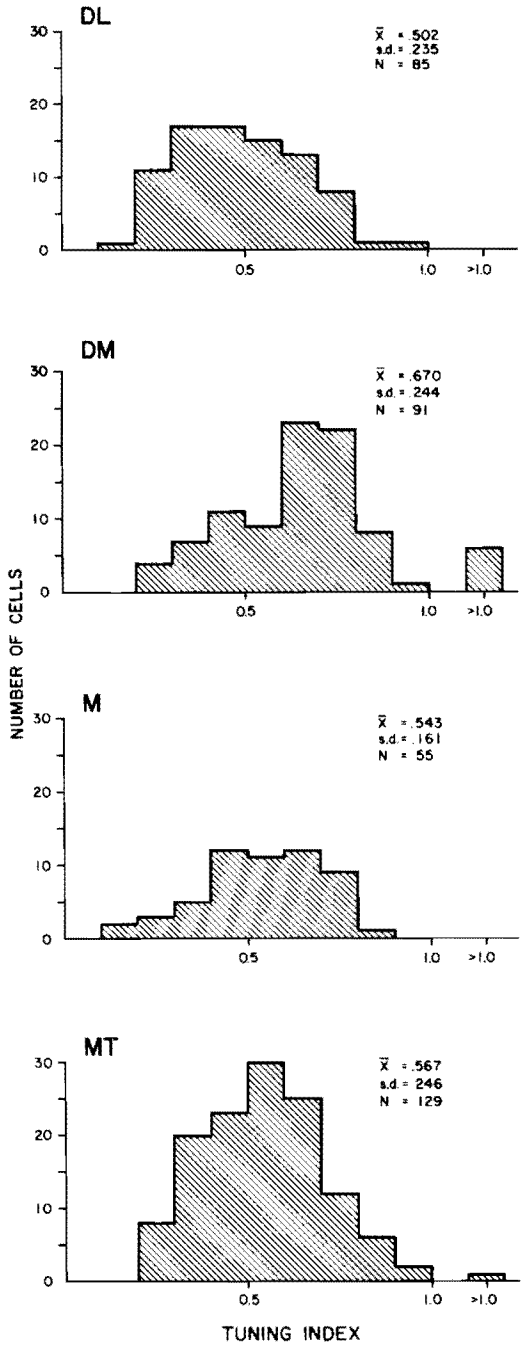

FIG. 4. Distribution of tuning indices for DM, DL, MT, and M. Cells in DM tend to be more sharply tuned than cells in the other areas. An analysis of variance was performed on these data (62). The value of S (Scheffe's multiple comparisons) for DM versus DL was 7.66; DM versus MT was 3.5; DM versus M was 3.41; P is very much smaller than 0.01 for the DM − DL difference and less than 0.02 for the DM − MT and DM − M differences (df = 3,351).

and directionality indices are shown for the four areas in Fig. 5. The bulk of the data for an area is clustered in a single region of its graph. The different location of this region in each graph is an indication of the differences among the areas. There is no evidence, in the form of multiple clusters on a graph, that would suggest multiple classes of cells within an area. Figure 5 also shows the small but significant correlation between directionality and tuning in DL ($r = 0.47$), DM ($r = 0.29$), and MT ($r = 0.34$).

Responses to moving spots

Direction series were also run with moving-spot stimuli to test direction sensitivity in the absence of an oriented stimulus (71). Many neurons in M and DM, most notably DM, responded quite poorly to small-spot stimuli. Fifteen of 23 DM cells tested with spots of various diameters showed summation up to or beyond 15° diameter, so disks up to 13° diameter were used to obtain good responses, although in every case the test spot was smaller than the tested neuron's mapped receptive field. Smaller spots evoked good responses from many DL cells (60) and were used to minimize the possibility that the disk stimulus acted as an approximate edge oriented orthogonal to its direction of movement. In every extrastriate area studied, the tuning indices for directions of spot movement (M, $\bar{x} = 0.462$; DM $\bar{x} = 0.449$; DL, $\bar{x} = 0.390$; MT, $\bar{x} = 0.450$) were significantly lower than the tuning indices for direction of bar movement (DM, DL, MT, $P < 0.005$; M, $P < 0.025$). Ninety-four of 120 cells were more sharply tuned to bars than to spots. The distribution of direction indices for bar stimuli was not significantly different from the distribution of direction indices for spot stimuli in any area.

Responses to flashed bars

The presentation of pseudorandomly ordered orientations of flashed bar stimuli was used to test orientation sensitivity in the absence of movement. Responses to flashed-bar stimuli were obtained from all areas, though some cells were unresponsive (9/106 cells) and others responded only weakly. A cell generally responded transiently to the onset of a bar flashed at the optimal orientation (as determined with a moving-bar stimulus), with a minority of cells (29/106) showing

TABLE 1. *Average response magnitude and signal-to-noise ratios*

	Moving Bar				Single Spot				Flashed Bar				Random Dots			
Area	*n*	$\bar{x}$	SD	S/N	*n*	$\bar{x}$	SD	S/N	*n*	$\bar{x}$	SD	S/N	*n*	$\bar{x}$	SD	S/N
Average best response, spikes/s																
DL	80	13.14	11.56	14.48	51	13.08	12.93	13.37	23	4.94	4.48	4.00	21	2.54	3.74	2.54
DM	89	14.12	15.57	13.13	25	8.85	11.64	8.82	20	8.16	7.12	15.31	13	3.89	4.63	2.50
M	56	20.65	17.18	13.42	32	21.08	23.73	7.50	22	12.03	10.09	7.80	21	21.74	19.46	10.30
MT	129	14.40	14.63	24.73	51	14.74	17.48	24.00	37	9.35	12.52	10.98	31	15.33	14.89	37.50
Best response to particular stimulus type																
Best response to moving bar																
DL					39	0.97	0.64		23	0.75	0.63		20	0.40	0.61	
DM					25	0.74	0.59		20	0.85	0.66		13	0.25	0.42	
M					24	0.78	0.56		21	0.62	0.43		19	0.83	0.51	
MT					43	0.93	0.63		34	0.66	0.65		31	1.13	0.59	

The signal-to-noise ratio S/N was calculated for each cell by dividing its mean discharge rate for the optimal-direction of movement or orientation by its average spontaneous activity. Median signal-to-noise ratios were used because cells with little or no spontaneous activity have very large signal-to-noise ratios and would tend to skew the mean ratios to a level that does not reflect their actual distributions.

an off-response. Occasionally (2/106) a cell was encountered that gave only an off-response. Only the responses to stimulus onset were used in the data analysis for this study. The tuning indices to stationary-bar stimuli were high, as shown in the histograms on the left of Fig. 6; the tuning indices were significantly higher in DM than in DL and M, and higher in MT than in DL. The right side of Fig. 6 shows the distributions of differences between a cell's flashed- and moving-bar tuning indices for each area. In each area, the average tuning index for stationary flashed bars was higher than for moving bars. This implies that the response of a cell to moving oriented bars is some combination of a broadly tuned response to direction of movement and a sharply tuned response to orientation. Orientation tuning was tested with flashed bars centered in two or more different regions of the receptive field of three neurons; the optimal orientation was independent of the position of the stimulus in the field. There was no signficant difference between the flashed-bar tuning of cells with high direction indices and cells with low direction indices.

Responses to moving random-dot patterns

For some cells, most frequently encountered in MT, the most effective stimulus among those tested was not a bar or spot, but an array of randomly spaced small dots moving in the same direction at a uniform velocity within a stationary window 40° in diameter. Outside the window, the field was uniformly illuminated. Figure 7 shows for cells in the four areas the comparison between the mean response to an optimally oriented bar stimulus moving in its best direction and the mean response to a random-dot array moving in its best direction. Sixteen of 31 MT cells tested with both random-dot arrays and the quantitatively determined optimal bar stimulus orientation and direction responded better to the array. The median signal-to-noise ratio for random-dot responses in MT was much higher than for the other areas and also was the highest for any class of stimuli tested in any area (see Table 1). Cells in M were also often quite responsive to the dot arrays (optimal stimulus for 6 of 21 tested cells), while DM (8/13) and DL (8/21) cells were frequently unresponsive.

Responses to stimulus velocity

The large majority of neurons in all four extrastriate areas fired best at a velocity in the 10–100°/s range. We chose the mean response rate during the stimulus sweep as our velocity-response measure; this represents a compromise between total spikes per sweep and peak rate measures, which emphasize low- and high-velocity responses, respectively (61). Typical examples of velocity tuning curves for a cell from DL and one from M are shown in Fig. 8. There was no

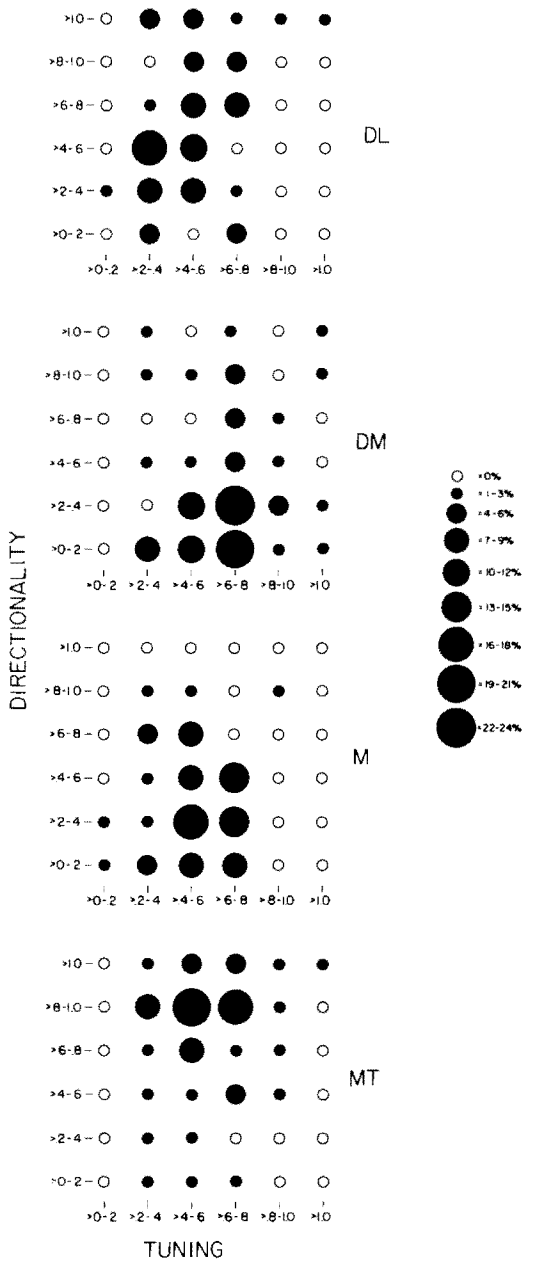

FIG. 5. Two-dimensional plots of tuning and directionality indices for cells in DL, DM, M, and MT. The size of a dot represents the percentage of cells that have appropriate values for the two indices. Each area has a concentration of cells in a single region of its graph; for example, DM cells generally have low direction indices and high tuning indices.

uniform shape of velocity tuning curves; the majority of cells were broadly tuned, but sharply tuned cells, low-pass responses, and high-pass responses were occasionally encountered. Overall, as displayed in Fig. 9, DL and MT contained a larger share of neurons that responded optimally at lower velocities around 10°/s, although both these areas contained some neurons that responded best at quite high velocities. Fourteen of 69 MT cells tested gave their optimal response at a velocity over 100°/s. Some MT cells fired well to a 500°/s stimulus, the highest velocity tested. DM neurons preferred intermediate velocities, and M cells preferred higher velocities. There was no correlation between the optimal velocity and the sharpness of tuning about that velocity ($r = 0.12$). Two neurons were encountered that did not respond to any smoothly moving stimulus but were excited by erratic small displacements produced under hand stimulus control.

Vertical organization of MT

Long penetrations nearly perpendicular to the cortical surface were made in MT to investigate systematic differences between superficial and deep cells in their orientation, direction, and random-array stimulus responses. The responses of a series of single neurons in a penetration in MT, which histological reconstruction showed to be perpendicular to the cortical surface and nearly parallel to the radial fibers, is illustrated in Fig. 10. The graphs on the right show the average response of each neuron to six different orientations each presented 10 times in pseudorandom order. The dotted line indicates the level of spontaneous activity for each neuron. Neuron *A* was broadly tuned; *B* through *K* all strongly preferred horizontally oriented bars; *L* was strongly inhibited by horizontal bars and thus was the negative complement of the other cells in the penetration. These data, together with other data we have obtained, suggest the presence of vertical columns of orientation-selective neurons in MT such as have been described for the primary visual area (V I) (37). The graphs on the left show the average response of each neuron to moving-bar stimuli crossing the receptive field in 12 different directions. In each case the bar was oriented perpendicular to the direction of movement. Neurons *A* through *F* responded optimally to a horizontally oriented bar approaching from 270° (straight down); neurons *G* through *K* responded optimally to a hori-

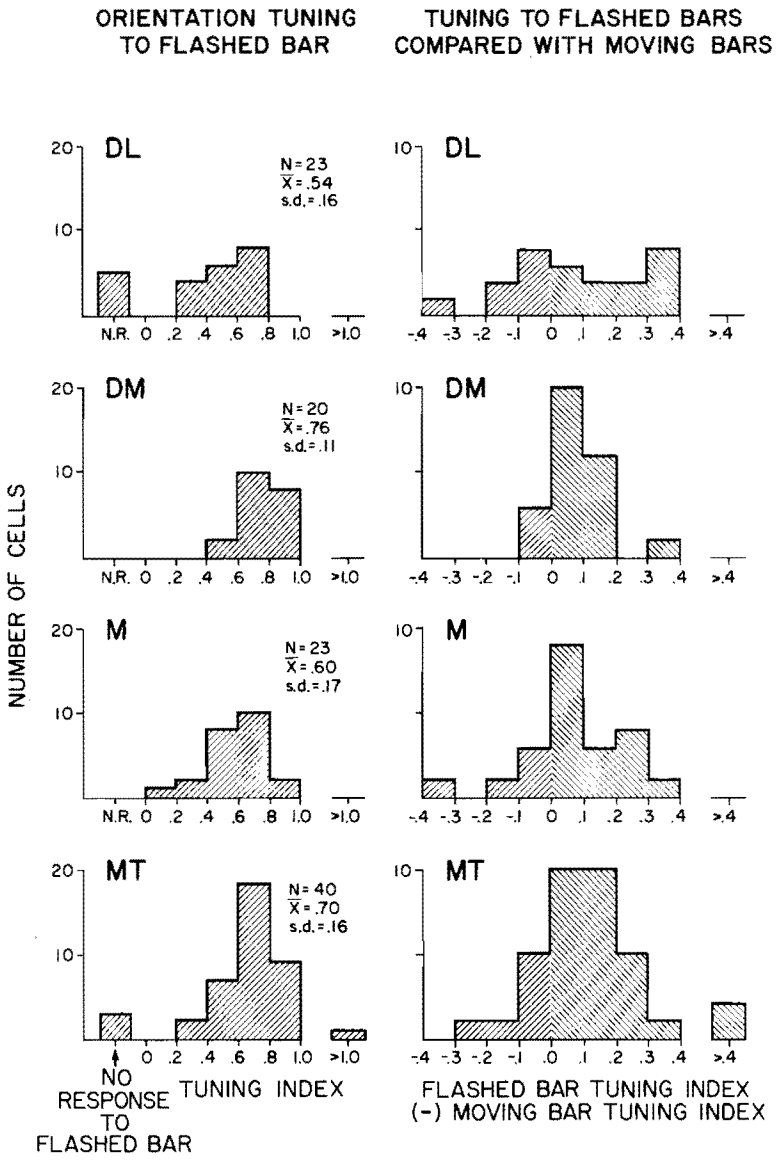

FIG. 6. *Left*: distributions of tuning indices to oriented stationary flashed-bar stimuli. The tuning indices were significantly higher in DM than in DL (S = 6.37) and M (S = 3.91), and higher in MT than DL (S = 4.28) ($P < 0.05$, df = 3,94). *Right*: distributions of the differences between each cell's flashed-bar and moving-bar tuning indices for each area.

zontally oriented bar approaching from 90° (straight up). One or more of these abrupt 180° shifts in preferred direction of movement have been observed in most of the long penetrations we have made in MT. These data suggest that groups of neurons with diametrically opposed preferred directions of movement lie juxtaposed within a larger system sharing the same orientation preference. We do not believe that the preferred direction is necessarily related to superficial versus deep layers, because we have observed other penetrations through all the layers in which all the cells had approximately the same preferred direction and orientation. While the preceding observations are generally characteristic of MT, some penetrations yielded less orderly patterns of organization.

The relative responsiveness to the array

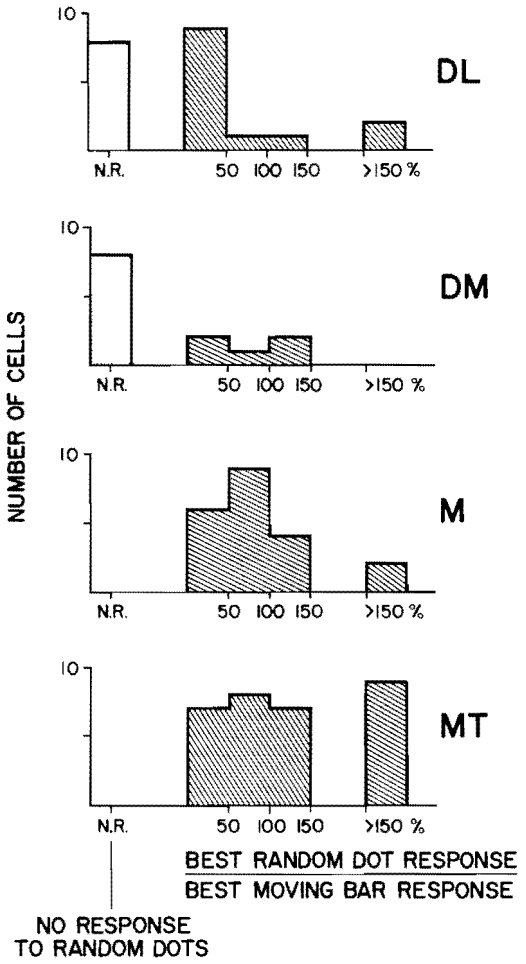

FIG. 7. Comparison between the response to an optimally oriented bar moving in its optimal direction at optimal velocity with the response to a moving array of random dots for DM, DL, MT, and M. The response to the moving array is expressed as a percentage of the response to the bar.

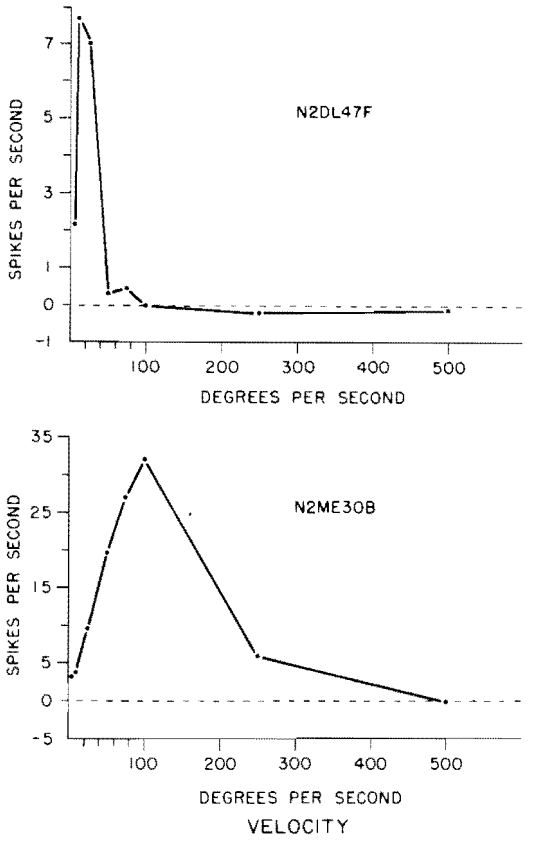

FIG. 8. Example of a cell in DL preferring a slow velocity (top) and a cell in M preferring a relatively high velocity (bottom). The response measure was mean spikes per second during the stimulus sweep.

of randomly spaced dots was greater in the deep layers of MT, as demonstrated by the significant correlation between electrode depth in the cortex and the maximal responses obtained to the random-dot array as a percentage of the best response to a bar stimulus ($r = 0.43$, $n = 31$, $P < 0.01$).

Eccentricity and receptive-field size

The magnification of central vision differs widely across the extrastriate areas (1) and the distribution of eccentricities of single-unit receptive fields from each area studied reflected the magnification in that area. The mean eccentricities (straight-line distances from the center of gaze) of receptive-field centers were: M, 36°; DM, 18°; DL, 13°; MT, 21°.

Extrastriate receptive fields varied widely in size and were generally much larger than striate fields (4). Excitatory receptive-field areas were usually computed from elliptical mapped regions, although rarely an odd shape such as a very long narrow rectangle or a kidney-shaped region was needed to encompass accurately the excitatory region. The mean receptive-field areas were: M, 768 deg^2, (SD 919 deg^2); DM, 257 deg^2 (SD 737 deg^2); DL, 229 deg^2 (SD 297 deg^2); MT, 258 deg^2 (SD 371 deg^2). Receptive-field area correlated well with eccentricity ($r = 0.62$ overall; M, $r = 0.74$; DM, $r = 0.62$; DL, $r = 0.48$; MT, $r = 0.67$). The large average receptive-field size of M neurons could be

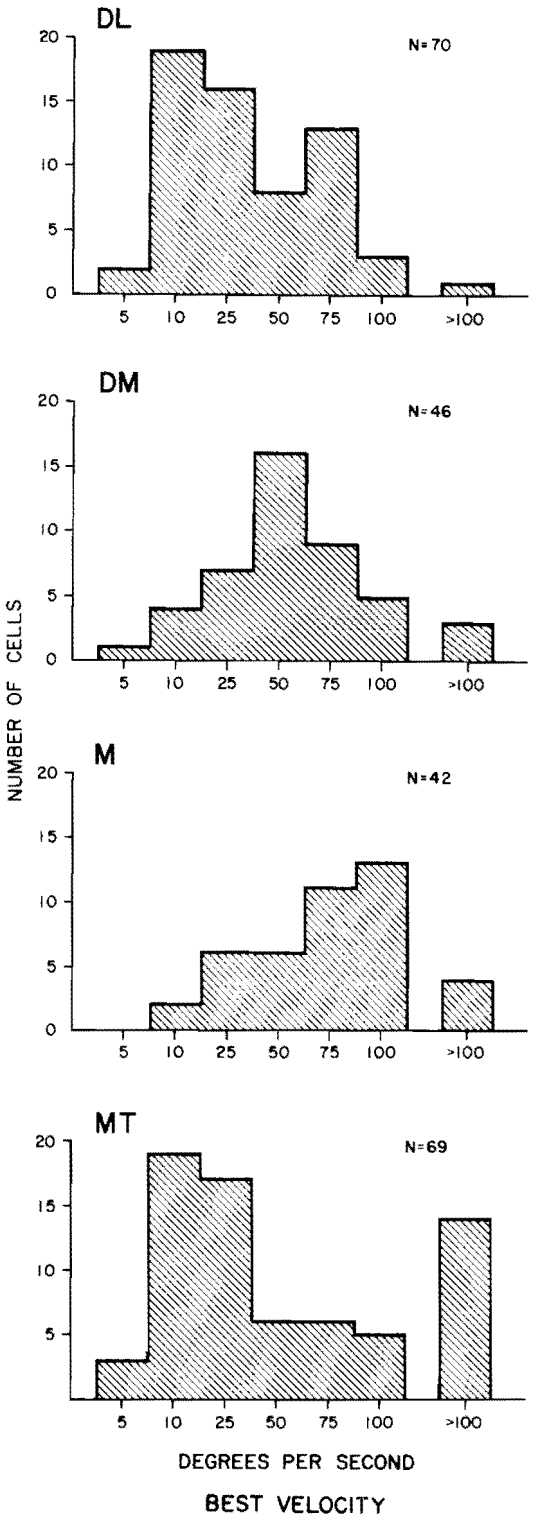

FIG. 9. Distributions of preferred velocities for neurons in DM, DL, MT, and M.

partially explained by the peripheral location of receptive fields in M (8). Correlating eccentricity with the direction index ($r = 0.07$), tuning index ($r = 0.17$), and best velocity ($r = 0.13$) showed that the differences in response properties across the four areas could not be attributed to eccentricity differences in the samples.

Summary comparison of response properties in DL, MT, DM, and M

A comparison of the functional indices for each area from this and a related study (60) are presented in Table 2. The high direction index for MT neurons compared with the significantly lower direction indices for DL, DM, and M indicates that MT neurons generally discriminate much better than cells in the other three areas the difference between movement in the preferred direction and movement in the direction 180° opposite. The orientation-tuning index indicates that neurons in DM are significantly better tuned to the orientation of moving bars than in the other three areas, but the difference is small. In each of the four areas the average tuning index for moving bars is lower than for stationary flashed bars. The random-dot index indicates that MT neurons respond significantly better to the moving random dot array than do cells in DL and DM. The dimensional-selectivity indices, which were taken from a related study (60), indicate that DL neurons generally are significantly better tuned than neurons in the other three areas for stimuli of particular spatial dimensions.

DISCUSSION

Significance of multiple cortical areas

There is strong evidence that some aspects of the response properties of neurons are segregated in the four extrastriate areas studied. Why has functional localization of response properties taken place? In attempting to develop computer analogues of visual perception, Marr (48) elaborated the principle of modular design. Marr stated that any large computation should be broken into a collection of smaller modules as independent as possible from one another. Otherwise, "the process as a whole becomes extremely difficult to debug or improve, whether by a

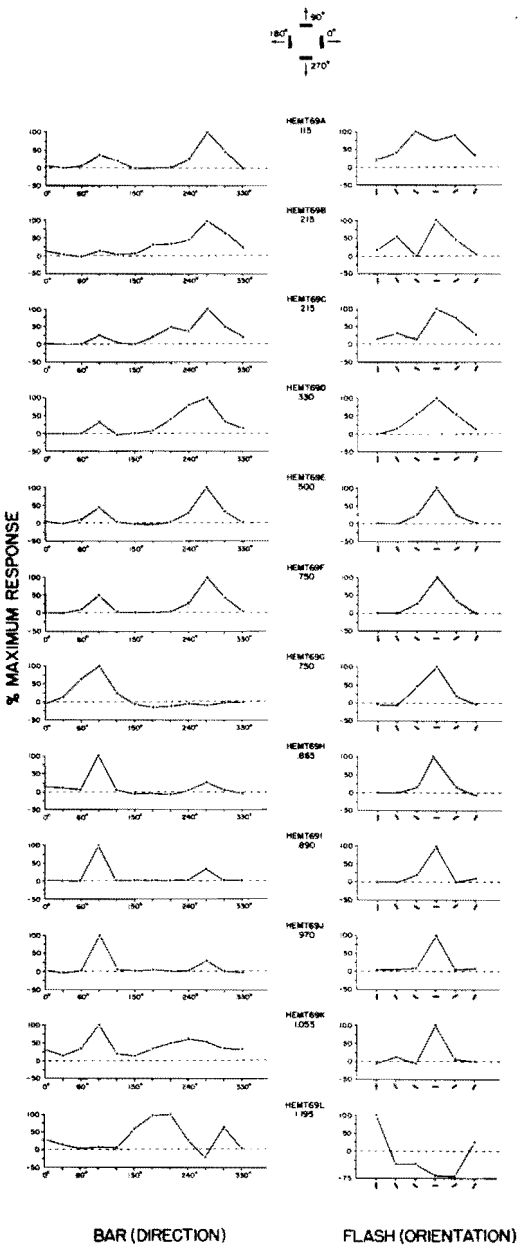

FIG. 10. Direction and orientation selectivity for a series of neurons recorded in a single penetration nearly perpendicular to the surface of MT. A pair of graphs is illustrated for each unit (*HEMT69A* through *L*). The depth beneath the surface at which each cell was recorded is given beneath each identifying number. An electrolytic lesion was made at the bottom of the microelectrode track. Histological reconstruction indicated that the penetration was perpendicular to the surface of MT and nearly parallel to the radial fibers. Cells *A* through *J* were located in layers II and III; cells *K* and *L* were located in layer IV. Graphs on the left illustrate the average response of each cell to five presentations of a 20 x 1° light bar at 12 different angles. *HEMT69A* through *F* preferred 270°; *HEMT69G* through *K* preferred 90°. Graphs on the right illustrate the average response of the cells to 10 presentations of a flashed bar at the orientations shown. All cells except the last preferred the horizontal orientation; the last was inhibited by horizontal bars. The direction of movement was 90° to the bar orientation, thus the preferred directions of 270° (down) and 90° (up) are consistent with the preferred horizontal orientation. The receptive-field centers were located an average of 16.6° below the horizontal meridian with a standard deviation of 0.9° and an average of 6.7° temporal to the vertical meridian with a standard deviation of 3.3°.

human designer or in the course of natural evolution, because a small change to improve one part has to be accompanied by many simultaneous changes elsewhere."

The formation of modules may have been produced by the replication of visual areas. The replication of existing structures appears to be a fundamental mechanism in evolution. The paleontologist Gregory (29) proposed that a common mechanism of evolution is the replication of body parts due to genetic mutation in a single generation, which is then followed in subsequent generations by the gradual divergence of structure and functions of the duplicated parts. The geneticist Bridges (13) proposed that chromosomal duplications would offer a reservoir of extra genes from which new ones might arise. It has been theorized that duplicated genes escape the pressures of natural selection operating on the original gene and thereby can accumulate mutations, which enable the new gene, through changes in its DNA sequence, to encode for a novel protein capable of assuming new functions (57). Many clear-cut examples of gene replication have been discovered (39, 45, 57) and DNA sequence homologies in replicated genes have recently been established (64). The same evolutionary advantages that hold for the replication of genes may also hold for the replication of visual areas (3, 6).

What then are the likely modular functions of the extrastriate areas studied here? Most neurons in all four areas are tuned for bar orientation as are the neurons in the primary visual cortex (37). This indicates that orientation selectivity is a main component of the basic plan for all the areas.

TABLE 2. *Comparison of response properties and central visual field representation in DL, MT, DM, and M*

Index	DL	DM	M	MT	Significant Differences
Directionality index	0.61	0.41	0.37	0.81	MT > DL > DM, M
Orientation-tuning index for flashed bars	0.54	0.76	0.60	.70	DM > DL, M MT > DL
Orientation-tuning index for moving bars	0.50	0.67	0.54	.56	DM > MT, M, DL
Best random-dot response / Best moving-bar response	0.40	0.25	0.83	1.13	MT > DM, DL
Dimensional selectivity index for length	0.59	0.28	0.27	0.31	DL > MT, DM, M
Most common preferred velocity, deg/s	10	50	100	10	
Area devoted to central 10° of visual field, %	73	22	4	10	

The direction, orientation, and moving random-dot indices are described in the text. The standard deviations for these indices are in the figures for each index. The dimensional selectivity index is taken from work published elsewhere (60). The index is calculated as: 1 − ((response to longest stimulus tested)/(response to optimal stimulus tested)). Length is the dimension orthogonal to the direction of movement. DL was also found to be significantly more selective for spot size than MT, DM, and M, and significantly more selective for width (dimension parallel to direction of movement) than MT (60). The percentage of each area devoted to the representation of the central 10° of the visual field was calculated from previous data (1, 3, 6–8).

MT neurons have supplemented this basic property of orientation selectivity with the further capability of discriminating direction of movement orthogonal to the preferred orientation. This capacity is present in a minority of neurons in the other areas, but is much better developed in MT. In addition, MT has the capacity for discriminating an entirely different type of stimulus, moving arrays of random dots. In primary visual cortex in the cat, responsiveness to moving random-dot arrays is characteristic of complex cells particularly in layer V, although these cells rarely respond better to visual texture than to an optimal bar as do the majority of cells in MT (33). This capacity to respond to random arrays requires a neural mechanism for integration over considerable distances in the visual cortex. A likely source of this integration is the convergence of input from primary visual cortex onto MT, particularly from the giant Meynert cells in layer V (52, 67; J. Wall, C.-S. Lin, and J. H. Kaas, personal communication). One of the outputs of MT is to the pontine nuclei (28) and this output is probably from the cells in the deep laminae, as is the case for the MT homologue in the macaque (26). Layer V corticopontine cells and pontine visual cells in the cat are similar to cells in the deep layers of MT; both are directionally selective and strongly respond to multiple-spot stimuli (10, 24). The entire output of the pontine nuclei is to the cerebellum, a major center for the control of body and eye movement.

In DL about 70% of the neurons are selective for the spatial dimensions of visual stimuli within excitatory receptive fields that are generally much larger than the preferred stimulus dimensions (see Table 2). The dimensional selectivity of DL cells is independent of the sign of contrast in the receptive field (equal to light-on-dark and dark-on-light stimuli), the amount of contrast (similar response over a 1.5 log unit change in intensity), and the position of the stimulus within the receptive field (60). DL neurons have a wide range of preferred sizes from 1 to 30° in length and from 0.25 to 7° in width, and these preferences appeared to be independent of each other when both dimensions were tested on the same cell (60). The dimensional selectivity of DL neurons suggests that DL contributes to form perception. This hypothesis is consistent with the observation that DL has the most expanded representation of the central visual

field (6) where the most acute recognition of form takes place and the recent discovery that DL is the main source of input to the inferotemporal cortex (84). Inferotemporal cortex has been strongly implicated in the analysis of complex visual stimuli and the learning of visual form discriminations (30, 31).

The most obvious distinctive feature of M is its relative emphasis on the representation of the peripheral visual field, which suggests that M might have a special role in functions in which peripheral vision is important, such as motion perception or orientation in space (8). However, the average direction index for area M neurons was the lowest of the four areas tested. DM is more sharply orientation selective than the other areas, but like the other areas is less sharply tuned to moving bars than to flashed stationary bars; DM neurons were the least responsive to the moving array of random dots.

Homologies

There is abundant evidence for similarities between the organization of visual cortex in the owl monkey and in other primate species; in some cases these similarities are so striking that the areas in question should be considered to be homologous. The most widely quoted definition is that of Simpson (66): "homology is resemblance due to inheritance from common ancestry." Three major criteria for the recognition of homology in the nervous system proposed by Campbell and Hodos (15) are the multiplicity of similarities, the fineness of detail of the similarities, and evidence from fossil lineages of common ancestry.

The most powerful case for homology of the extrastriate visual areas is that of MT and similar visual areas in other primate species. This homology has been pointed out by several workers (31, 77, 78, 83). The argument for homology is based on similar location, myeloarchitecture, topography, distinctive anatomical connectivity, and visual response properties. Owl monkey MT is a striate-receptive region of dense myelination coextensive with an orderly map of the visual hemifield (3). A corresponding striate-receptive region of dense myelination coextensive with a similar map of the visual field has been reported in galago (9, 74), marmoset (68, 69), and macaque (23, 50, 80, 82). A major source of input to MT in the owl monkey is from V I cells in or near the stria of Gennari and from the giant cells of Meynert located in the lower part of layer V (personal communication, J. Wall, C.-S. Lin, and J. H. Kaas). A similar projection occurs in marmoset (67) and macaque (46) from striate cortex cells in the stria of Gennari and the giant Meynert cells. MT is the only known extrastriate cortical target of the Meynert cells (47). Directional selectivity is the principal characteristic of owl monkey MT cell responses, and this has been shown to be true for the corresponding region of the macaque (50, 89). The presence of these extensive and detailed similarities in three superfamilies of primates, including primates from both infraorders, indicates that MT probably existed in the early primates ancestral to all living primates.

In a recent paper, Zeki (92) contends that MT in the owl monkey and the striate projection zone of the superior temporal sulcus in the macaque are not homologous. His contention is based in part on the assertion that insufficient anatomical similarities exist for the areas to be considered homologous. However, Zeki's discussion of structural similarities does not include any mention of the distinctive heavy myelination of the deeper layers of owl monkey and macaque MT, nor does he mention the precise similarity in anatomical projection to MT from striate cortex. While Zeki found that owl monkey MT cells shared with macaque MT cells the major property of directional selectivity, his argument rests primarily on his contention that there are major differences in the visual response properties of owl monkey and macaque MT cells. He cites three differences: *a*) the dependence of owl monkey MT cell responses on the presence of a near optimal stimulus and the relative absence of such dependence in the macaque, *b*) the presence of orientation selectivity in most owl monkey MT cells and its relative rarity in macaque MT cells, and *c*) the presence of a wide variety of binocular interaction effects on owl monkey MT cells but not on macaque cells.

Zeki states that the stimulus requirements of owl monkey MT cells "made the initial penetrations frustrating, with cell after cell either not responding, or responding in a

vague manner." This was not the case under our experimental conditions. While we found many examples of orientation, length, width, and/or diameter selectivity (59), we also found in the same cells that any of a wide variety of nonoptimal, nonoriented stimuli evoked vigorous responses and these responses had impressive signal-to-noise ratios. In fact, a field of randomly scattered dots was the optimal stimulus for the majority of MT cells, and most cells were also well driven by a single spot (see Table 1). This contradiction between our results and Zeki's may be due to differences between the two preparations, possibly the use of Vetame-ketamine tranquilization versus barbiturate anesthesia. The results of our flashed oriented-bar presentations clearly support Zeki's claim of orientation selectivity in owl monkey MT cells. However, we do not know whether orientation selectivity would be revealed in macaque MT with the flashed-bar test, and without a description of Zeki's orientation-selectivity testing procedure, it is difficult to evaluate the differences he reports. In both owl monkey and macaque MT, Zeki found the majority of cells to be driven equally by stimulation of either eye. The presence of a minority of cells having more specialized binocular interactions in the owl monkey MT suggests a greater emphasis on binocular processing.

In view of the preponderance of other evidence, the differences in the orientation selectivity and binocular interactions of owl monkey and macaque MT cells are not compelling arguments against their homology. Homology refers to similarity due to common ancestry, not identity. In this context, the optic tectum can serve as a useful example. The visuotopic organization of the optic tectum in primates differs from that found in all other vertebrates (1). In addition, in macaque monkeys directional cells are rare or absent in the optic tectum (19, 27, 65), while in cats and squirrel monkeys (42, 72), these make up a significant percentage of cells in the ventral part of the superficial layers. In spite of these differences, few would argue that the optic tecta of these animals did not arise from the same structure in their common ancestors.

In our present state of knowledge, it is more difficult to establish clear-cut homologies for the other visual areas found beyond V II in the owl monkey. However, evidence for the homology of several areas is emerging. The principal input to inferotemporal visual cortex in the owl monkey is DL (84). In macaques a region adjacent to MT is a main input to inferotemporal cortex (20). This region, like DL in the owl monkey, emphasizes the representation of the central visual field (21). MT in both owl monkeys and macaques does not appear to project to inferotemporal cortex. The position of DL between MT and V II in owl monkeys is topographically similar to V4 in macaques. However, the boundaries of V4 have not been completely mapped, and it may constitute more than one area (80, 88). Neurons in V4 have been reported to be color selective, but the percentage of neurons showing this attribute in V4 has ranged from 100 to 32% in different studies, and a recent report suggests that color processing in V4 is substantially similar to the color selectivity found in foveal V I and V II (43).

Another potential homology is that of the ventral posterior (VP) areas of the owl monkey and the macaque (54, 56; see Fig. 1). These areas are similar in that they both are long narrow strips that lie immediately anterior to V II on the ventral surface, with this common border corresponding to a representation of the horizontal meridian. In both monkeys, the anterior border of VP corresponds to a discrete band of degeneration following section of the corpus callosum. In both monkeys, the visual-field representation in VP appears to be limited to the upper quadrant with the more central portions represented laterally and the more peripheral portions medially. The establishment of potential homologies for DM and M awaits further investigation.

Outside of primates it is much more difficult to establish homologies. The last common ancestor of the different mammalian orders lived no more recently than the late Cretaceous period more than 60 million years ago (63). This ancestral mammal had only a very limited development of its neocortex (40). In addition, the adaptive radiation of mammals into different ecological niches with widely divergent behavioral specializations serves to make very difficult the discovery of diagnostic similarities among

potentially homologous cortical areas in different mammalian orders.

In the cat, area 21a and area 19 (V3) occupy positions that bear some topographic similarities to MT and DL; area 19 partially wraps around area 21a, and the two areas adjoin each other along a common border representing the vertical meridian in the lower field (75). The dimensionally selective properties of DL neurons resemble some of the higher order-hypercomplex cells described by Hubel and Wiesel (35) for V III in the cat, although these cells constituted only a small portion of their sample (35). Area 21a, while bearing some topographic similarity to MT, contains a representation of only the central 30° of the contralateral hemifield. The striate-receptive lateral suprasylvian region in the cat has been suggested as a potential homologue of MT (1). The neurons in the lateral suprasylvian region typically are directionally selective and thus resemble MT in this respect (36, 71). The neurons have also been reported to have dimensionally selective properties similar to DL (14). The establishment of homologies with this region in the cat is further complicated by the recent discovery that it contains six visual areas (58).

In the gray squirrel, the temporal posterior area (Tp) is a possible homologue of MT. Tp lies adjacent to part of the vertical meridian representation in area 19, and thus these areas bear a topographic similarity to MT and DL (32). In addition, Tp, like MT, is densely myelinated with a laminar pattern similar to MT (41). In a similar location in the rabbit, there is a striate-receptive visual area that has been suggested as a possible homologue of MT, but the response properties of the neurons in this area in the rabbit differ markedly from MT (17, 49).

While similarities in the organization of other mammals is less well documented, multiple representations of the visual field exist in many other species (78). Multiple representations also occur in other sensory systems; for example, the auditory (38) and somatosensory (51; see Fig. 1). The ubiquitous nature of multiple representations and the evidence for the localization of response properties to these areas argues that functional localization is a successful evolutionary solution to the problems of complex information processing.

ACKNOWLEDGMENTS

We thank Leslie Wolcott for drawing the figures.

This research was supported by National Institutes of Health Grants NS-00178, NS-12131, and GM-07737; National Science Foundation Grant BNS-77-15605, and the Pew Memorial Trust.

Present address of W. T. Newsome: Laboratory of Sensorimotor Research, National Eye Institute, Bethesda, MD 21205.

Received 15 July 1980; accepted in final form 30 September 1980.

REFERENCES

1. ALLMAN, J. M. Evolution of the visual system in the early primates. In: *Progress in Psychobiology and Physiological Psychology*, edited by J. M. Sprague and A. N. Epstein. New York: Academic, 1977, vol. 7, p. 1–53.
2. ALLMAN, J. M., CAMPBELL, C. B. G., AND MCGUINNESS, E. The dorsal third tier area in *Galago senegalensis*. *Brain Res.* 179: 355–361, 1979.
3. ALLMAN, J. M., AND KAAS, J. H. A representation of the visual field in the caudal third of the middle temporal gyrus of the owl monkey (*Aotus trivirgatus*). *Brain Res.* 31: 84–105, 1971.
4. ALLMAN, J. M. AND KAAS, J. H. Representation of the visual field in striate and adjoining cortex of the owl monkey (*Aotus trivirgatus*). *Brain Res.* 35: 89–106, 1971.
5. ALLMAN, J. M. AND KAAS, J. H. The organization of the second visual area (VII) in the owl monkey: a second order transformation of the visual hemifield. *Brain Res.* 76: 247–265, 1974.
6. ALLMAN, J. M. AND KAAS, J. H. A crescent-shaped cortical visual area surrounding the middle temporal area (MT) in the owl monkey (*Aotus trivirgatus*). *Brain Res.* 81: 199–213, 1974.
7. ALLMAN, J. M. AND KAAS, J. H. The dorsomedial cortical visual area: a third tier area in the occipital lobe of the owl monkey (*Aotus trivirgatus*). *Brain Res.* 100: 473–487, 1975.
8. ALLMAN, J. M. AND KAAS, J. H. Representation of the visual field on the medial wall of occipital-parietal cortex in the owl monkey. *Science* 191: 572–575, 1976.
9. ALLMAN, J. M., KAAS, J. H., AND LANE, R. H. The middle temporal visual area (MT) in the bushbaby, *Galago senegalensis*. *Brain Res.* 57: 197–202, 1973.
10. BAKER, J. F., GIBSON A., GLICKSTEIN, G., AND STEIN, J. Visual cells in the pontine nuclei of the cat. *J. Physiol. London* 255: 415–433, 1976.

11. BAKER, J. F., MIEZIN, F. M., MYERSON, J., NEWSOME, W. T., PETERSEN, S. E., AND ALLMAN, J. M. Quantitative response properties of neurons in the dorsomedial area (DM), a third tier visual area in the owl monkey. *Soc. Neurosci. Abstr.* 3: 552, 1977.
12. BARLOW, H. B., HILL, R. M., AND LEVICK, W. R. Retinal ganglion cells responding selectively to direction and speed of image motion in the rabbit. *J. Physiol. London* 173: 377–407, 1964.
13. BRIDGES, C. B. Salivary chromosome maps. *J. Hered.* 26: 60–64, 1935.
14. CAMARDA, R. AND RIZZOLATTI, G. Visual receptive fields in the lateral suprasylvian area (Clare-Bishop area) of the cat. *Brain Res.* 101: 427–443, 1976.
15. CAMPBELL, C. B. G. AND HODOS, W. The concept of homology and the evolution of the nervous system. *Brain Behav. Evol.* 3: 353–367, 1970.
16. CHAN-PALAY, V., PALAY, S. L., AND BILLINGS-GAGLIARDI, S. M. Meynert cells in the primate visual cortex. *J. Neurocytol.* 3: 631–658, 1974.
17. CHOW, K. L., DOUVILLE, A., MASCETTI, G., AND GROBSTEIN, P. Receptive field characteristics of neurons in a visual area of rabbit temporal cortex. *J. Comp. Neurol.* 171: 135–146, 1976.
18. CRAGG, B. G. The topography of the afferent projections in circumstriate visual cortex of the monkey studied by the Nauta method. *Vision Res.* 9: 733–747, 1969.
19. CYNADER, M. AND BERMAN, N. Receptive-field organization of monkey superior colliculus. *J. Neurophysiol.* 35: 187–201, 1972.
20. DESIMONE, R., FLEMING, J., AND GROSS, C. G. Prestriate afferents to inferior temporal cortex: an HRP study. *Brain Res.* In press.
21. DESIMONE, R. AND GROSS, C. G. Visual areas in the temporal cortex of the macaque. *Brain Res.* 178: 363–380, 1979.
22. FERNALD, R. AND CHASE, R. An improved method for plotting retinal landmarks and focusing the eyes. *Vision Res.* 11: 95–96, 1971.
23. GATTAS, R. AND GROSS, C. G. A visuotopically organized area in the posterior superior temporal sulcus of the macaque. *Ann. Meeting Assoc. Res. Vision Opthalmol. 1979*, p. 184.
24. GIBSON, A., BAKER, J., MOWER, G., AND GLICKSTEIN, M. Corticopontine cells in area 18 of the cat. *J. Neurophysiol.* 41: 484–495, 1978.
25. GILBERT, C. D. AND KELLY, J. P . The projections of cells in different layers of the cat's visual cortex. *J. Comp. Neurol.* 163: 81–105, 1975.
26. GLICKSTEIN, M., COHEN, J., DIXON, B., GIBSON, A., HOLLINS, M., LA BOSSIERE, E., AND ROBINSON, F. Corticopontine visual projection in the macaque monkey. *J. Comp. Neurol.* 190: 209–230, 1980.
27. GOLDBERG, M. E. AND WURTZ, R. H. Activity of superior colliculus in behaving monkey. I. Visual receptive fields of single neurons. *J. Neurophysiol.* 35: 542–559, 1972.
28. GRAHAM, J., LIN, C.-S., AND KAAS, J. H. Subcortical projections of six visual cortical areas in the owl monkey, *Aotus trivirgatus*. *J. Comp. Neurol.* 187: 557–580, 1979.
29. GREGORY, W. K. Reduplication in evolution. *Q. Rev. Biol.* 10: 272–290, 1935.
30. GROSS, C. G. Visual functions of inferotemporal cortex. In: *Handbook of Sensory Physiology*, VII/3 B, edited by R. Jung. Berlin: Springer, 1973, p. 451–482.
31. GROSS, C. G., BRUCE, C. J., DESIMONE, R., FLEMING, J., AND GATTAS, R. Three visual areas of the temporal lobe. In: *Multiple Cortical Areas*, edited by C. N. Woolsey. Englewood Cliffs, NJ: Humana. In press.
32. HALL, W. C., KAAS, J. H., KILLACKEY, H., AND DIAMOND, I. T. Cortical visual areas in the grey squirrel (*Sciurus carolinensis*): a correlation between cortical evoked potential maps and architectonic subdivisions. *J. Neurophysiol.* 34: 437–452, 1971.
33. HAMMOND, P. AND MACKAY, D. M. Differential responsiveness of simple and complex cells in cat striate cortex to visual texture. *Exp. Brain Res.* 30: 106–154, 1977.
34. HUBEL, D. H. AND WIESEL, T. N. Receptive fields, binocular interaction and functional architecture in the cat's visual cortex. *J. Physiol. London* 160: 106–154, 1962.
35. HUBEL, D. H. AND WIESEL, T. N. Receptive fields and functional architecture in two non-striate visual areas (18 and 19) of the cat. *J. Neurophysiol.* 28: 229–289, 1965.
36. HUBEL, D. H. AND WIESEL, T. N. Visual area of the lateral suprasylvian gyrus (Clare-Bishop area) of the cat. *J. Physiol. London* 202: 251–260, 1969.
37. HUBEL, D. H. AND WIESEL, T. N. Functional architecture of macaque monkey visual cortex. *Proc. R. Soc. London Ser. B* 198: 1–59, 1977.
38. IMIG, T. J., RUGGERO, M. A., KITZES, L. M., JAVEL, E., AND BRUGGE, J. F. Organization of auditory cortex in the owl monkey (*Aotus trivirgatus*). *J. Comp. Neurol.* 171: 111–128, 1977.
39. INGRAM, V. M. *The Hemoglobins in Genetics and Evolution*. New York: Columbia Univ. Press, 1963.
40. JERISON, H. *Evolution of the Brain and Intelligence*. New York: Academic, 1973.
41. KAAS, J. H., HALL, W. C., AND DIAMOND, I. T. Visual cortex of the grey squirrel (*Sciurus carolinensis*): architectonic subdivisions and connections from the visual thalamus. *J. Comp. Neurol.* 145: 273–306, 1972.
42. KADOYA, S., WOLIN, L. R., AND MASSOPUST, L. C. Photically evoked unit activity in the tectum opticum of the squirrel monkey. *J. Comp. Neurol.* 158: 319–338, 1972.
43. KRUGER, J. AND GOURAS, P. Spectral selectivity of cells and its dependence on slit length in monkey visual cortex. *J. Neurophysiol.* 43: 1055–1069, 1980.
44. KUYPERS, H. G. J. M., SZWARCBART, M. K., MISHKIN, M., AND ROSVOLD, H. E. Occipito-temporal cortico-cortical connections in the rhesus monkey. *Exp. Neurol.* 11: 245–262, 1965.
45. LEWIS, E. B. Pseudoallelism and gene evolution. *Cold Spring Harbor Symp. Quant. Biol.* 16: 159–174, 1951.
46. LUND, J. S., LUND, R. D., HENDRICKSON, A. E., BUNT, A. H., AND FUCHS, A. F. The origin of ef-

ferent pathways from the primary visual cortex, area 17, of the macaque monkey as shown by retrograde transport of horseradish peroxidase. *J. Comp. Neurol.* 164: 287–304, 1976.

47. LUND, J. S., HENRY, G. H., MACQUEEN, C. L., AND HARVEY, A. R. Anatomical organization of the primary visual cortex (area 17) of the cat. a comparison with area 17 of the macaque monkey. *J. Comp. Neurol.* 184: 599–618, 1979.
48. MARR, D. Early processing of visual information. *Phil. Trans. R. Soc. London Ser. B* 275: 484–519, 1976.
49. MATHERS, L. H., DOUVILLE, A., AND CHOW, K. L. Anatomical studies of a temporal visual area in the rabbit. *J. Comp. Neurol.* 171: 147–156, 1977.
50. MAUNSELL, J. H. R., BIXBY, J. L., AND VAN ESSEN, D. C. The middle temporal (MT) area in the macaque: architecture, functional properties and topographic organization. *Soc. Neurosci. Abstr.* 5: 796, 1979.
51. MERZENICH, M. M., KAAS, J. H., SUR, M., AND LIN, C.-S. Double representation of the body surface within cytoarchitectonic areas 3b and 1 in SI in the owl monkey (*Aotus trivirgatus*). *J. Comp. Neurol.* 181: 41–74, 1978.
52. MONTERO, V. M. Patterns of connections from the striate cortex to cortical visual areas in superior temporal sulcus of macaque and middle temporal gyrus of owl monkey. *J. Comp. Neurol.* 189: 45–55, 1980.
53. MYERS, R. E. Commissural connections between occipital lobes of the monkey. *J. Comp. Neurol.* 118: 1–16, 1962.
54. NEWSOME, W. T. AND ALLMAN, J. M. The interhemispheric connections of visual cortex in the owl monkey, *Aotus trivirgatus*, and the bushbaby, *Galago senegalensis*. *J. Comp. Neurol.* 194: 209–233, 1980.
55. NEWSOME, W. T., BAKER, J. F., MIEZIN, F. M., MYERSON, J., PETERSEN, S. E., AND ALLMAN, J. M. Functional localization of neuronal response properties in extrastriate visual cortex of the owl monkey. *Ann. Meeting Assoc. Res. Vision Ophthalmol. 1978*, p. 174.
56. NEWSOME, W. T., MAUNSELL, J. H. R., AND VAN ESSEN, D. C. Areal boundaries and topographic organization of the ventral posterior area (VP) of the macaque monkey. *Soc. Neurosci. Abstr.* 6: 579, 1980.
57. OHNO, S. *Evolution by Gene Duplication.* New York: Spring, 1970.
58. PALMER, L. A., ROSENQUIST, A. C., AND TUSA, R. J. The retinotopic organization of lateral suprasylvian visual areas in the cat. *J. Comp. Neurol.* 177: 237–256, 1978.
59. PETERSEN, S. E., BAKER, J. F., ROCKLAND, K. S., AND ALLMAN, J. M. Visual response properties of single neurons in the dorsolateral crescent (DL) in the owl monkey: selectivity for stimulus size, direction, and orientation. *Soc. Neurosci. Abstr.* 5: 803, 1979.
60. PETERSEN, S. E., BAKER, J. F., AND ALLMAN, J. M. Dimensional selectivity of neurons in the dorsolateral visual area of the owl monkey. *Brain Res.* 197: 507–511, 1980.
61. PETTIGREW, J. D., NIKARA, T., AND BISHOP, P. O. Responses to moving slits by single units in cat striate cortex. *Exp. Brain Res.* 6: 373–390, 1968.
62. POLLARD, J. H. *A Handbook of Numerical and Statistical Techniques.* Cambridge: Cambridge University Press, 1977.
63. ROMER, A. S. *Vertebrate Paleontology.* Chicago: Univ. of Chicago Press, 1966.
64. ROYAL, A., GARAPIN, A., CAMI, B., PERRIN, F., MANDEL, J. L., LEMEUR, M., BRÉGÉGÈGRE, F., GANNON, F., LEPENNEC, J. P., CHAMBON, P., AND KOURILSKY, P. The ovalbumin gene region: common features in the organisation of three genes expressed in chicken oviduct under hormonal control. *Nature London* 279: 125–132, 1979.
65. SCHILLER, P. H. AND KOERNER, F. Discharge characteristics of single units in superior colliculus of the alert rhesus monkey. *J. Neurophysiol.* 34: 920–936, 1971.
66. SIMPSON, G. G. *Principles of Animal Taxonomy.* New York: Columbia Univ. Press, 1961.
67. SPATZ, W. B. An efferent connection of the solitary cells of Meynert. A study with horseradish peroxidase in the marmoset, *Callithrix*. *Brain Res.* 92: 450–455, 1975.
68. SPATZ, W. B. Topographically organized reciprocal connections between areas 17 and MT (visual area of the superior temporal sulcus) in the marmoset (*Callithrix jacchus*). *Exp. Brain. Res.* 27: 559–572, 1977.
69. SPATZ, W. B. AND TIGGES, J. Experimental-anatomical studies on the "middle temporal visual area (MT)" in primates. I. Efferent corticocortical connections in the marmoset (*Callithrix jacchus*). *J. Comp. Neurol.* 146: 451–563, 1972.
70. SPATZ, W. B., TIGGES, J., AND TIGGES, M. Subcortical projections, cortical associations, and some intrinsic interlaminar connections of the striate cortex in the squirrel monkey (*Saimiri*). *J. Comp. Neurol.* 140: 155–174, 1970.
71. SPEAR, P. D. AND BAUMANN, T. P. Receptive-field characteristics of single neurons in lateral suprasylvian visual area of the cat. *J. Neurophysiol.* 38: 1403–1420, 1975.
72. STERLING, P. AND WICKELGREN, B. G. Visual receptive fields in the superior colliculus of the cat. *J. Neurophysiol.* 32: 1–15, 1969.
73. TALBOT, S. A. A lateral localization in cat's visual cortex. *Federation Proc.* 1: 84, 1942.
74. TIGGES, J., TIGGES, M., AND KALAHA, C. S. Efferent connections of area 17 in galago. *Am. J. Phys. Antropol.* 38: 393–398, 1973.
75. TUSA, R. J. AND PALMER, L. A. The retinotopic organization of areas 20 and 21 in the cat. *J. Comp. Neurol.* 193: 147–164, 1980.
76. TUSA, R. J., PALMER, L. A., AND ROSENQUIST, A. C. The retinotopic organization of the visual cortex in the cat. *Soc. Neurosci. Abstr.* 1: 52, 1975.
77. UNGERLEIDER, L. G. AND MISHKIN, M. The striate projection zone in the superior temporal sulcus of *Macaca mulatta*: location and topographic organization. *J. Comp. Neurol.* 188: 347–366, 1979.
78. VAN ESSEN, D. C. Visual cortical areas. In: *Ann. Rev. Neurosci.* vol. 2, edited by W. M. Cowan. Palo Alto: Annual Reviews, 1979, p. 227–263.
79. VAN ESSEN, D. C., MAUNSELL, J. H. R., AND BIXBY, J. L. The organization of extrastriate visual

areas in the macaque monkey. In: *Multiple Cortical Areas*, edited by C. N. Woolsey. Englewood Cliffs, NJ: Humana. In press.

80. VAN ESSEN, D. C. AND ZEKI, S. M. The topographic organization of rhesus monkey prestriate cortex. *J. Physiol. London* 277: 193–226, 1978.
81. WATKINS, D. W., WILSON, J. R., SHERMAN, S. M., AND BERKLEY, M. A. Receptive field organization: further differences between simple and complex cells. *Ann. Meeting Assoc. Res. Vision Ophthalmol., 1975*, p. 17.
82. WELLER, R. E. AND KAAS, J. H. Connections of striate cortex with the posterior bank of the superior temporal sulcus in macaque monkeys. *Soc. Neurosci. Abstr.* 4: 650, 1978.
83. WELLER, R. E. AND KAAS, J. H. Cortical and subcortical connections of visual cortex in primates. In: *Multiple Cortical Areas*, edited by C. N. Woolsey. Englewood Cliffs, NJ: Humana. In press.
84. WELLER, R. E. AND KAAS, J. H. Connections of the dorsolateral visual area (DL) of extrastriate visual cortex of the owl monkey (*Aotus trivirgatus*). *Soc. Neurosci. Abstr.* 6: 580, 1980.
85. WOLBARSHT, M. L., MACNICHOL, E. F., AND WAGNER, H. G. Glass insulated platinum microelectrode. *Science* 132: 1309–1310, 1960.
86. WRIGHT, M. J. Visual receptive fields of cells in a cortical area remote from the striate cortex of the cat. *Nature London* 223: 973–975, 1969.
87. ZEKI, S. M. Representation of central visual fields in prestriate cortex of monkey. *Brain Res.* 14: 271–291, 1969.
88. ZEKI, S. M. Colour coding in the superior temporal sulcus of rhesus monkey visual cortex. *Brain Res.* 53: 422–427, 1973.
89. ZEKI, S. M. Functional organization of a visual area in the posterior bank of the superior temporal sulcus of the rhesus monkey. *J. Physiol. London* 236: 549–573, 1974.
90. ZEKI, S. M. Uniformity and diversity of structure and function in rhesus monkey prestriate cortex. *J. Physiol. London* 277: 273–290, 1978.
91. ZEKI, S. M. Functional specialization in the visual cortex of the rhesus monkey. *Nature London* 274: 423–428, 1978.
92. ZEKI, S. M. The response properties of cells in the middle temporal area (area MT) of owl monkey visual cortex. *Proc. R. Soc. London Ser. B* 207: 239–248, 1980.